Electronic Supplementary Material (ESI) for CrystEngComm.

Supporting Information

Joining of trinuclear $(CuL)_2M$ (M = Mn^{II} and Cd^{II}) nodes by 1,3- and 1,4-benzenedicarboxylate linkers: Positional isomeric effect on co-crystallization

Sabarni Dutta[a], Subrata Jana[a], Prithwish Mahapatra[a], Antonio Bauzá[b], Antonio Frontera[b,*] Ashutosh Ghosh[a,*]

[a]*Department of Chemistry, University College of Science, University of Calcutta, 92, A.P.C. Road, Kolkata 700 009, India, E-mail address: ghosh_59@yahoo.com*

[b]*Departament de Química, Universitat de les Illes Balears, Crta. de Valldemossa km 7.5, 07122, Palma (Baleares), Spain*

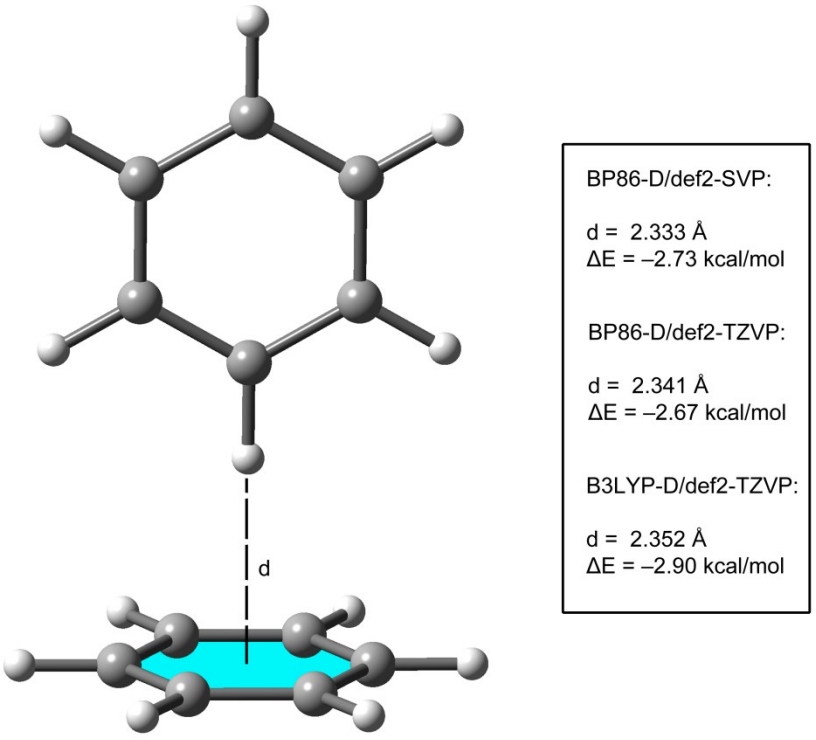

Fig. S1. Representative picture of a T-shape benzene dimer.

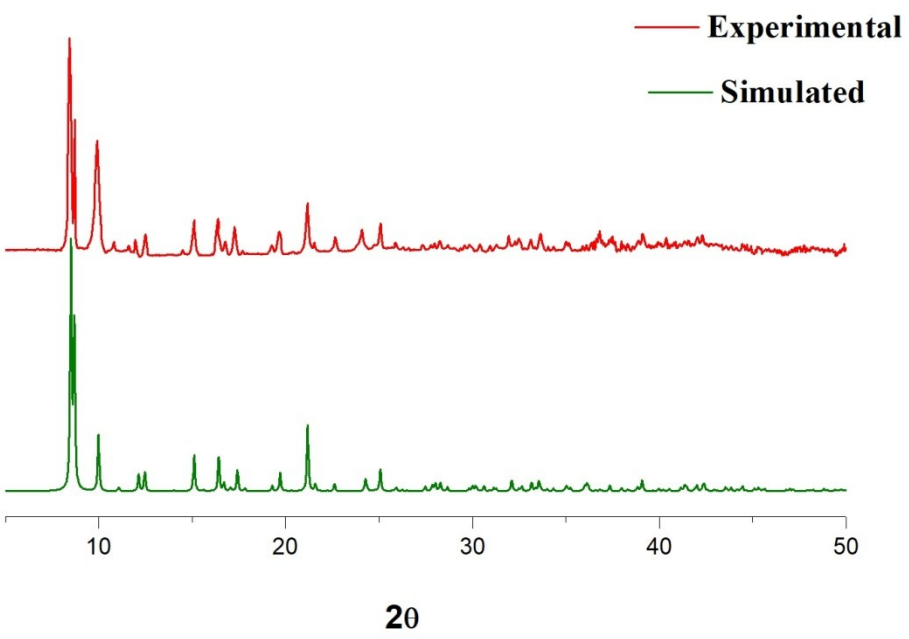

Fig. S2. Representative powder diffractogram of complex **1**.

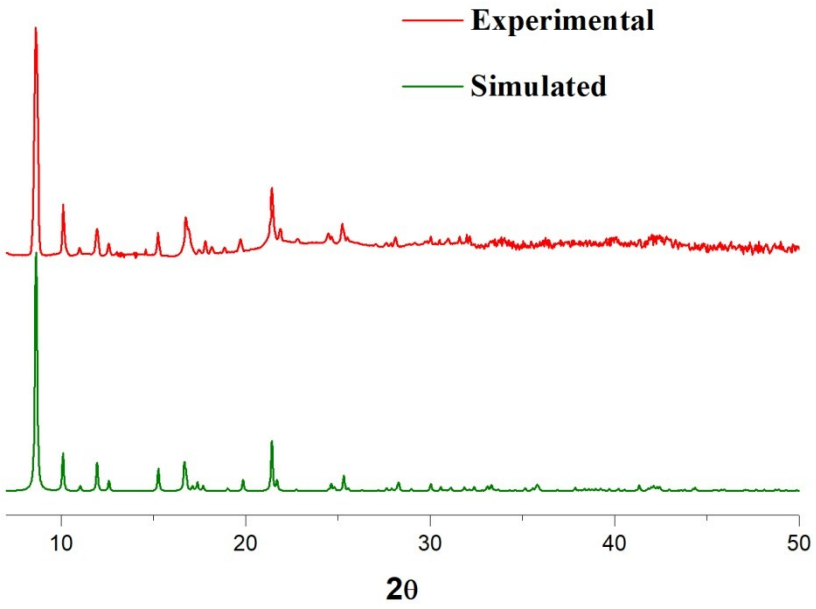

Fig. S3. Representative powder diffractogram of complex **2**.

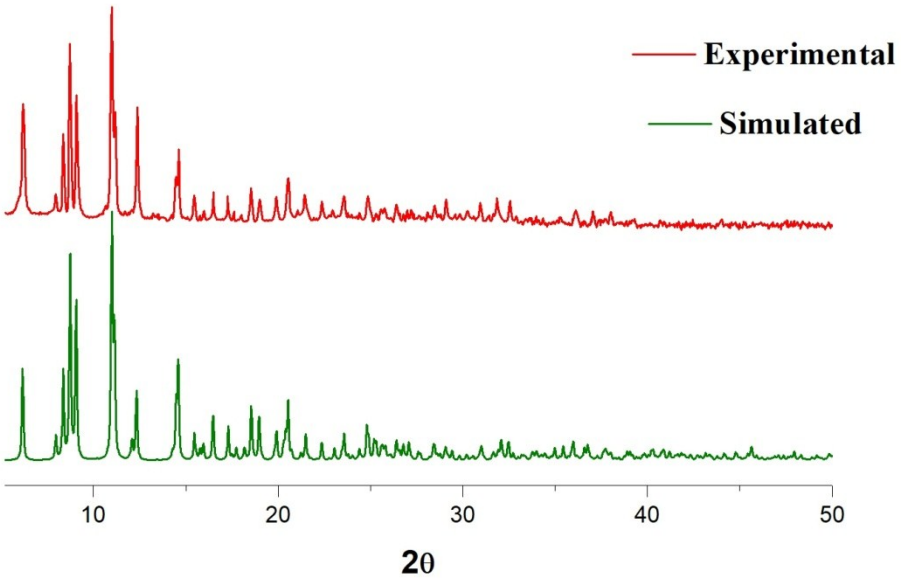

Fig. S4. Representative powder diffractogram of complex **3**.

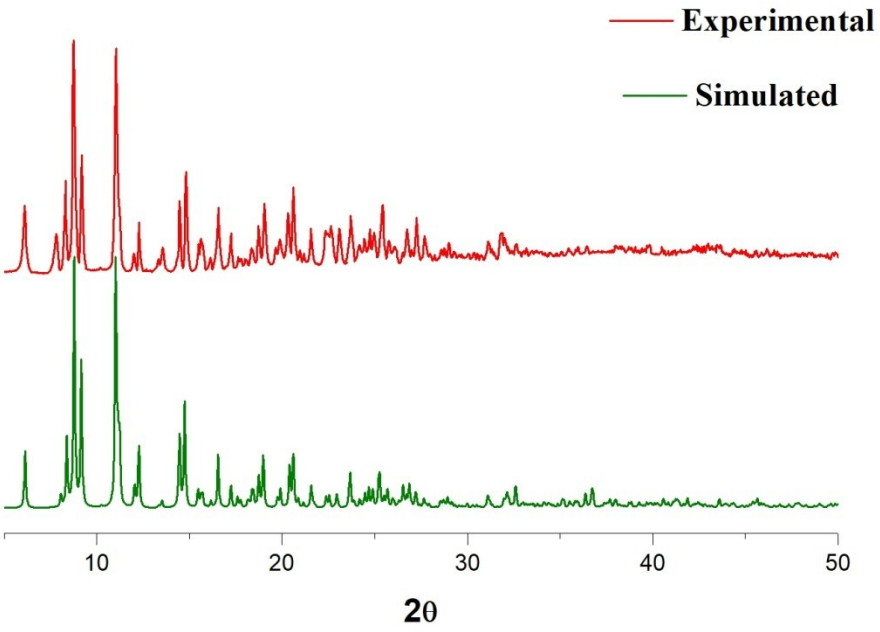

Fig. S5. Representative powder diffractogram of complex **4**.

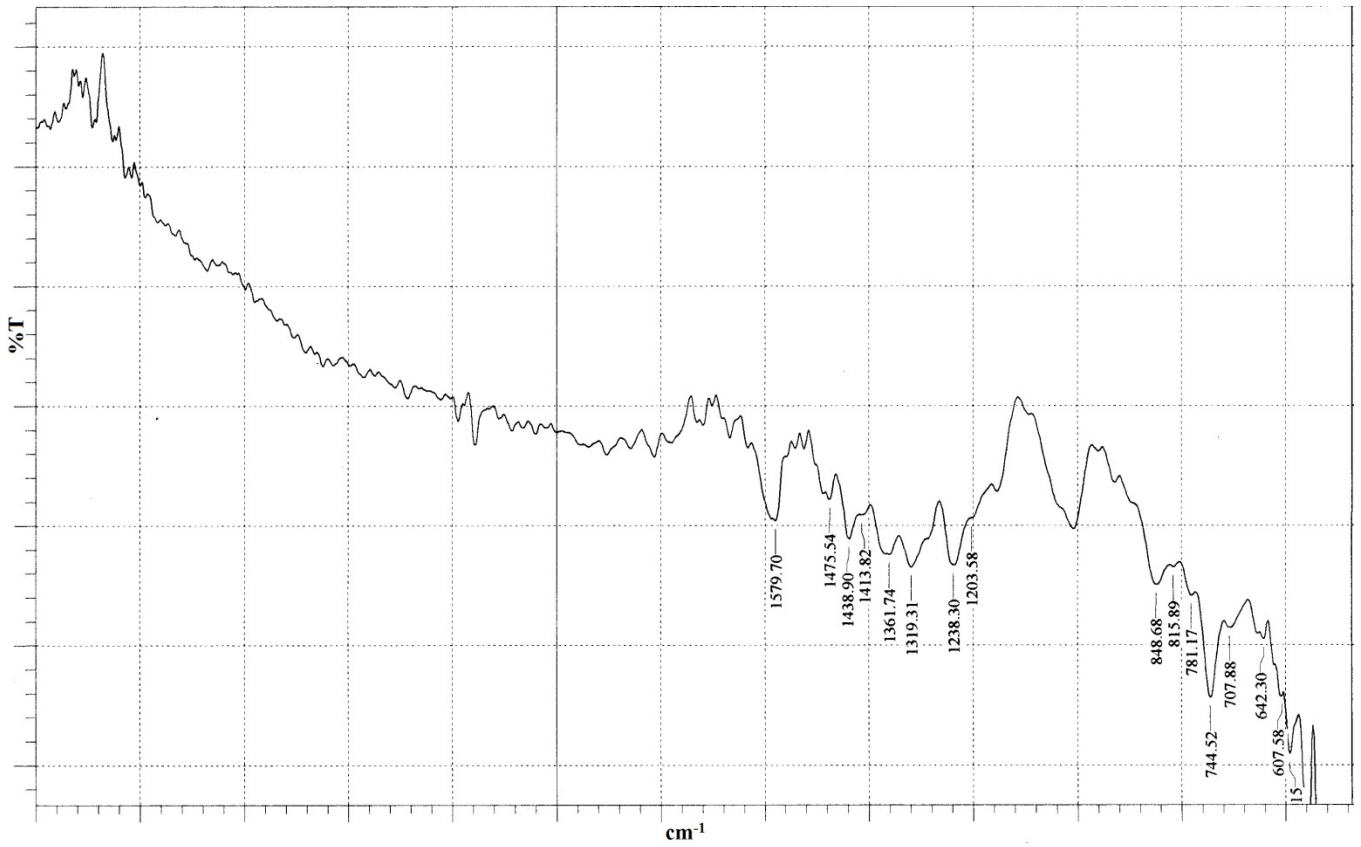

Fig. S6. FT- IR spectrum (ATR Technique) of complex **1**.

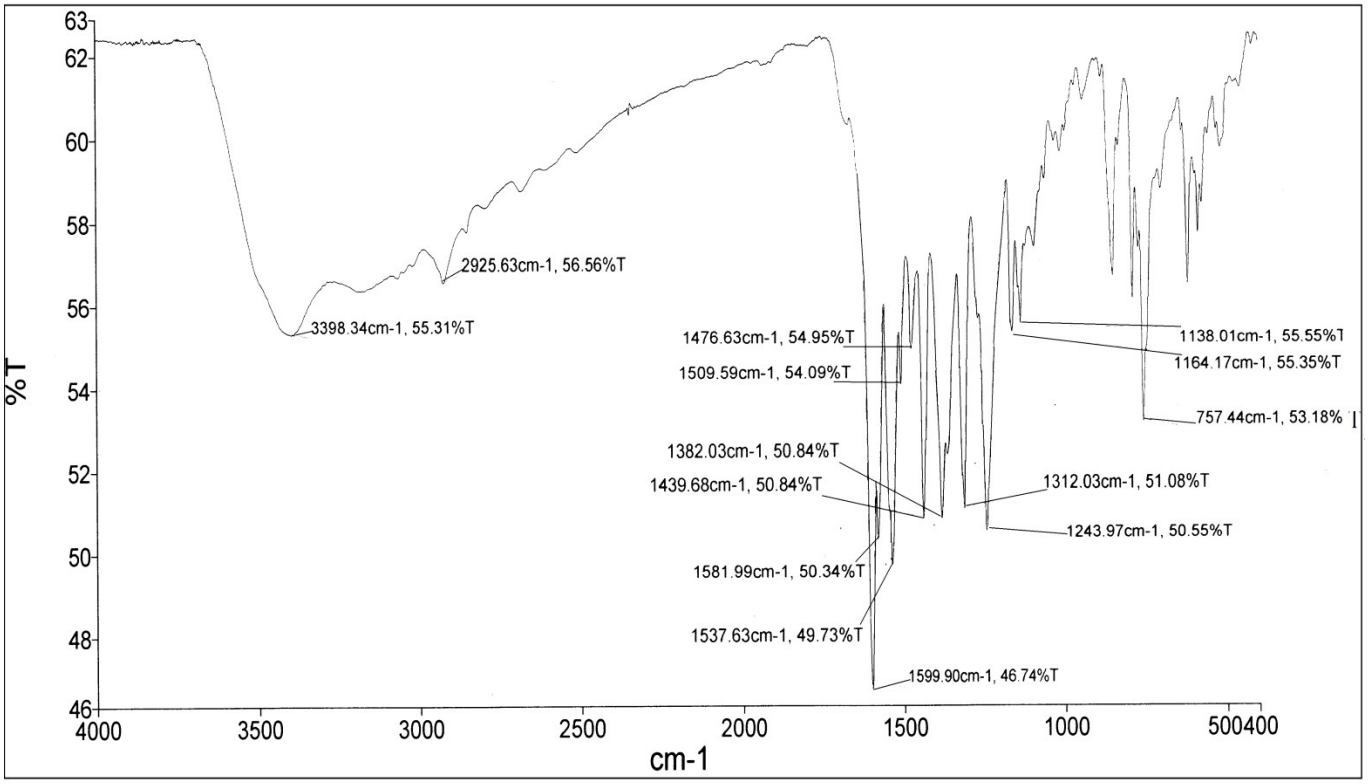

Fig. S7. FT-IR Spectrum (KBr pellet Technique) of complex **1**.

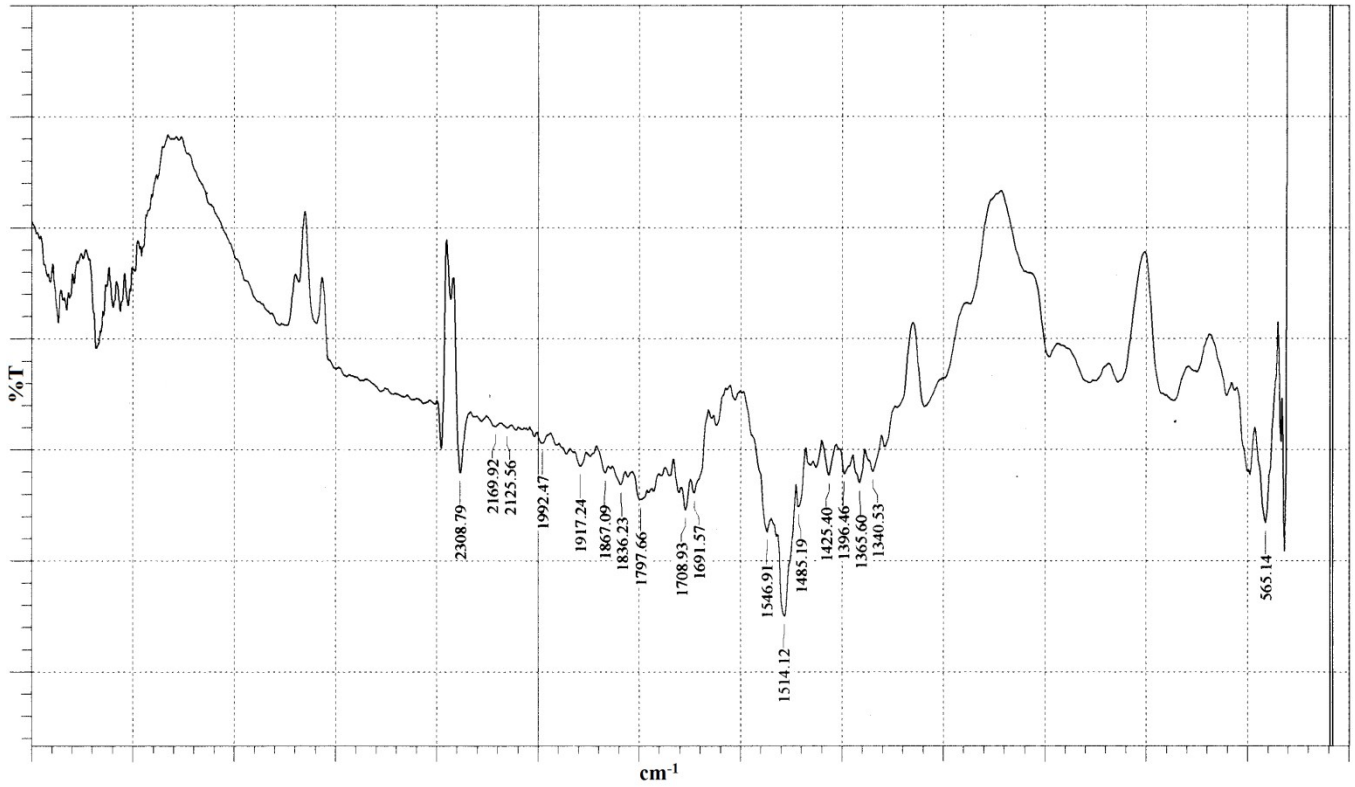

Fig. S8. FT- IR spectrum (ATR Technique) of complex **2**.

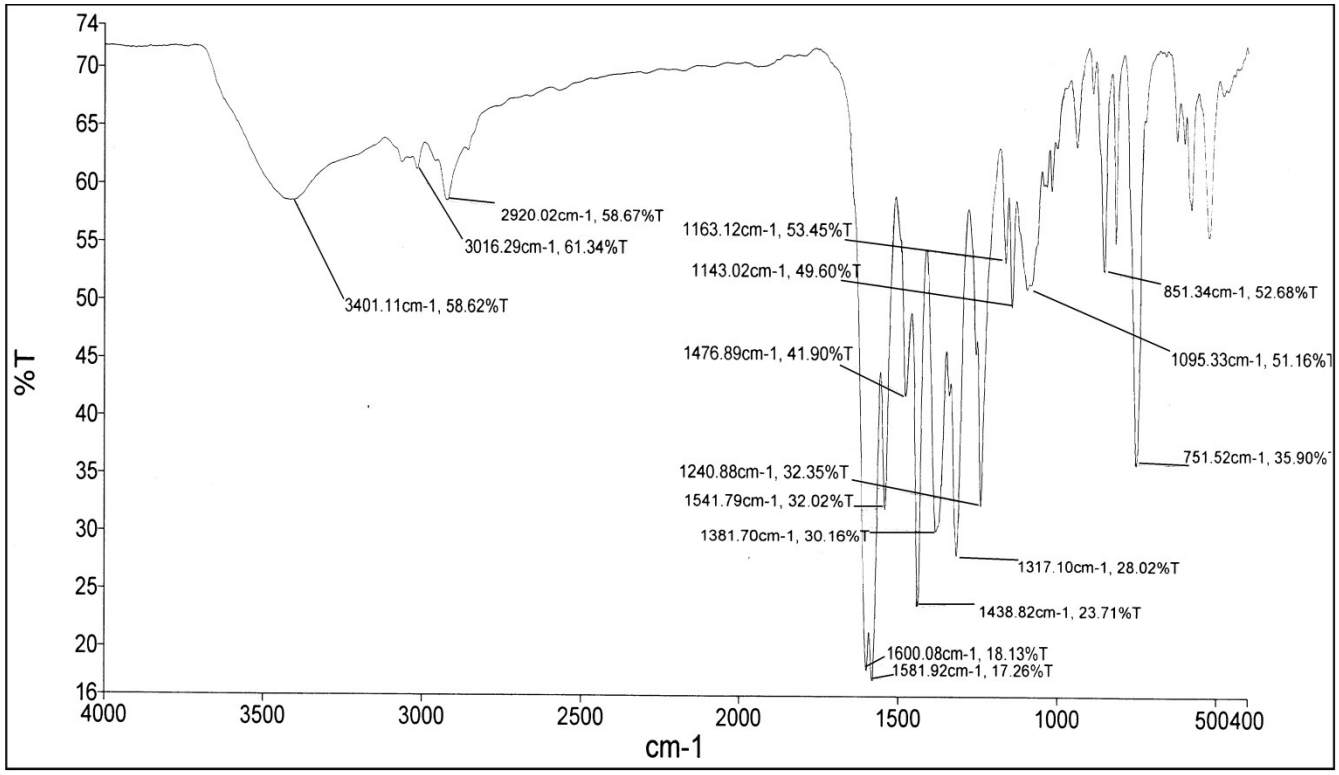

Fig. S9. FT- IR spectrum (KBr pellet Technique) of complex **2**.

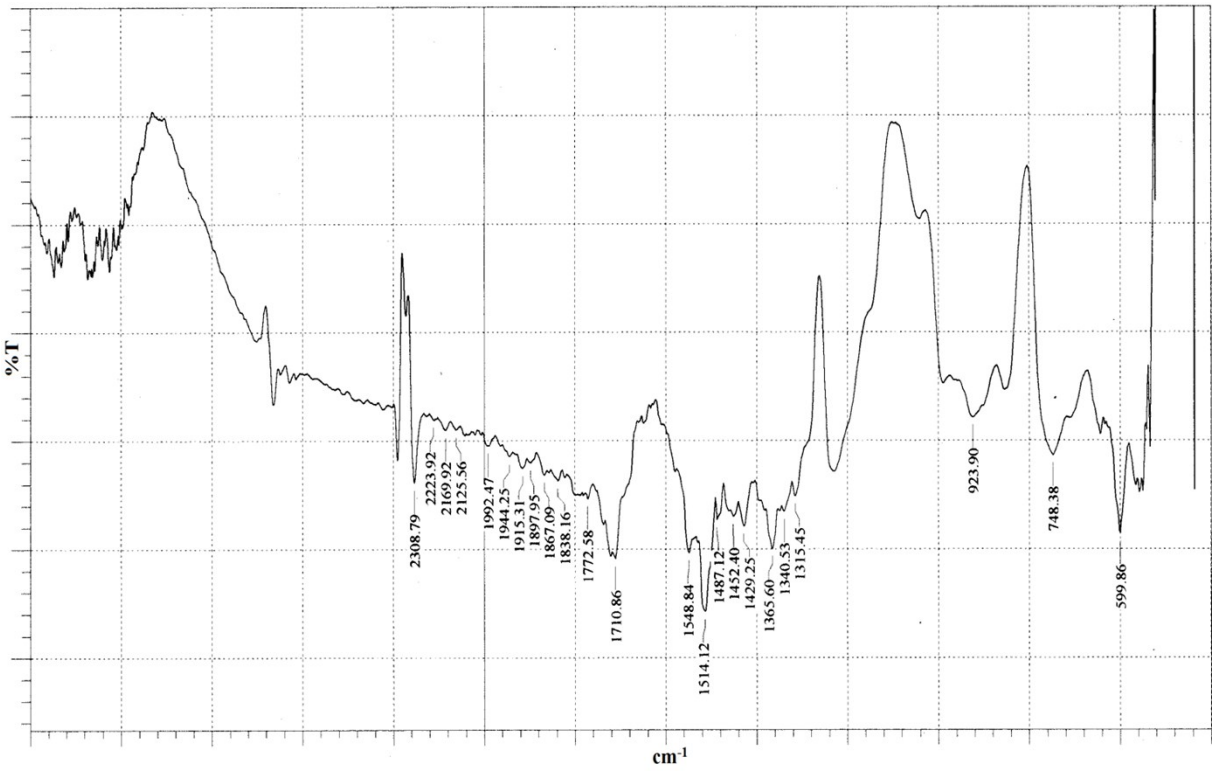

Fig. S10. FT- IR spectrum (ATR Technique) of complex **3**.

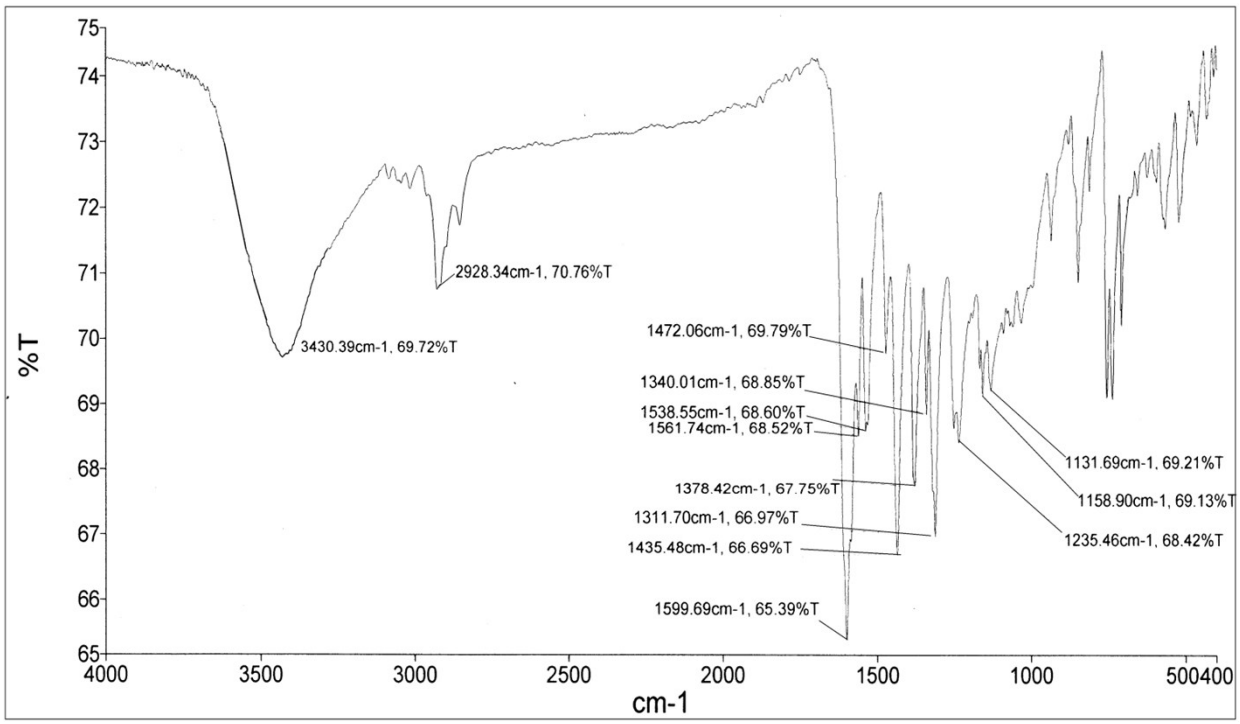

Fig. S11. FT- IR spectrum (KBr pellet Technique) of complex **3**.

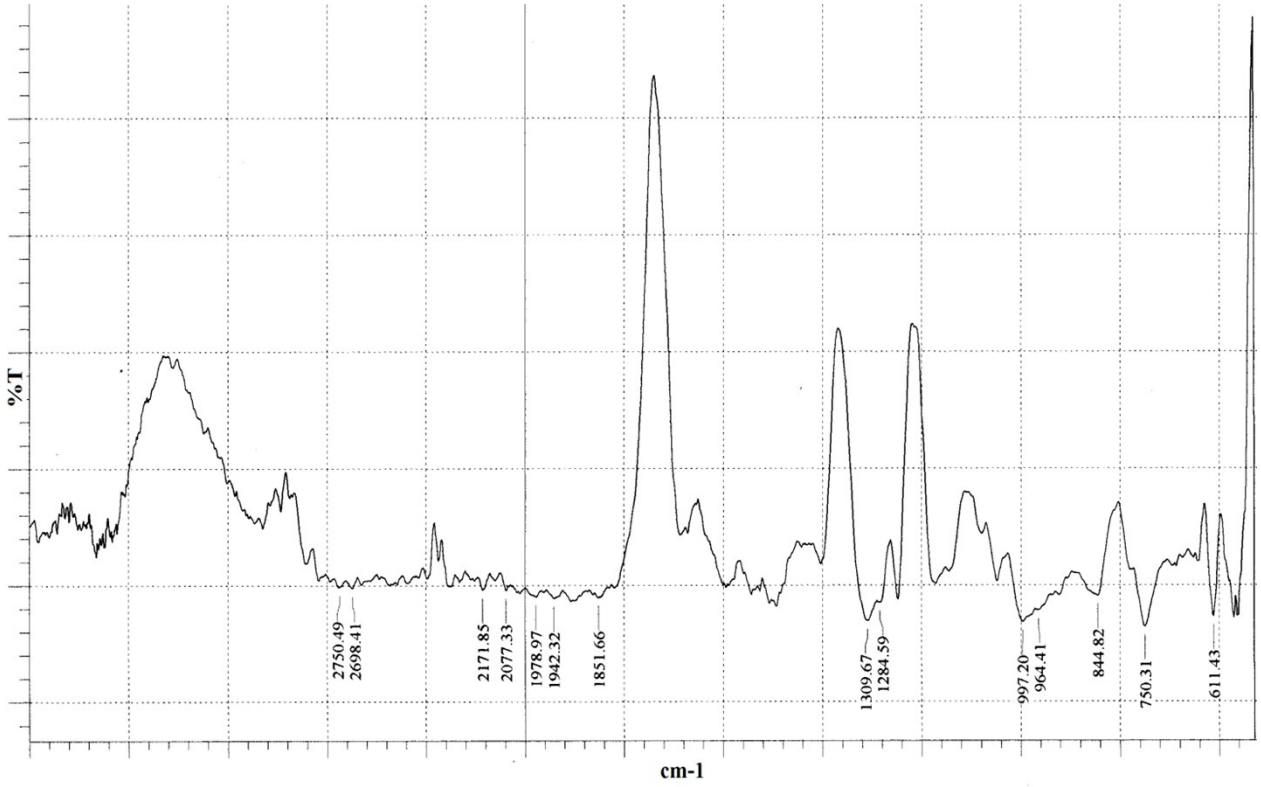

Fig. S12. FT- IR spectrum (ATR Technique) of complex **4**.

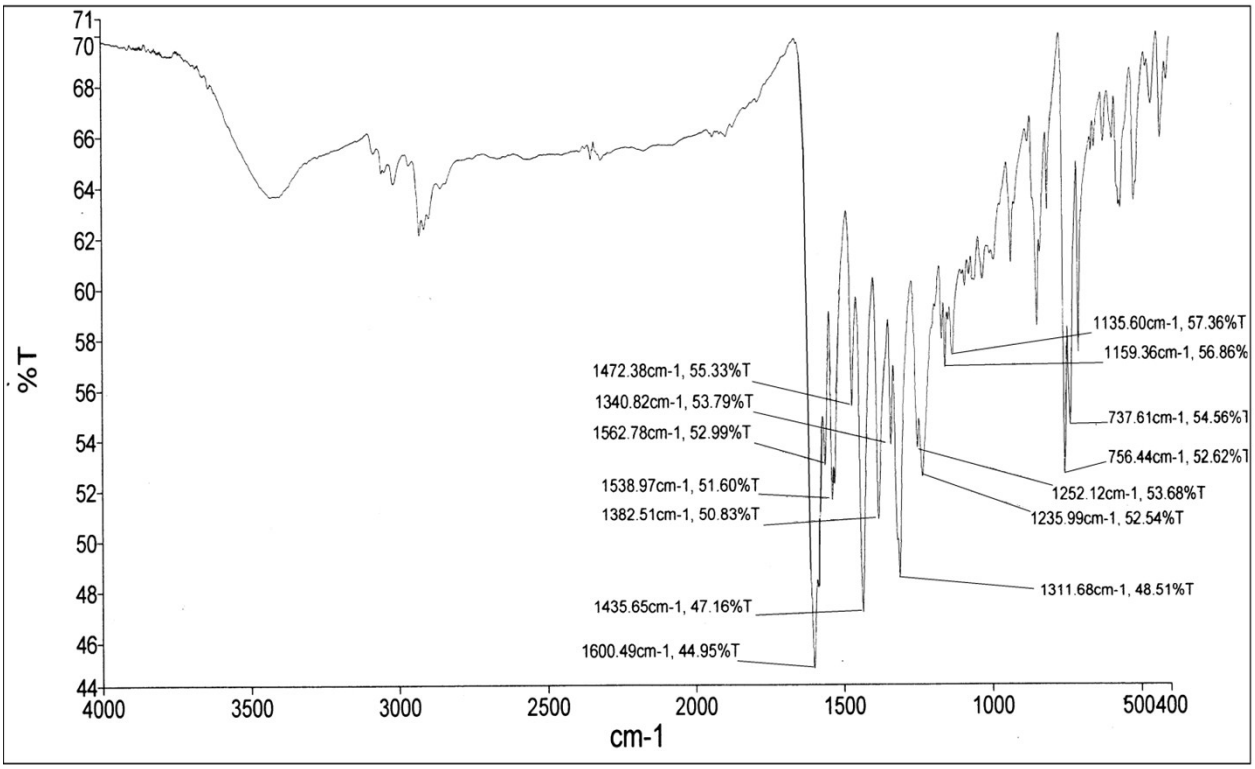

Fig. S13. FT- IR spectrum (ATR Technique) of complex **4**.

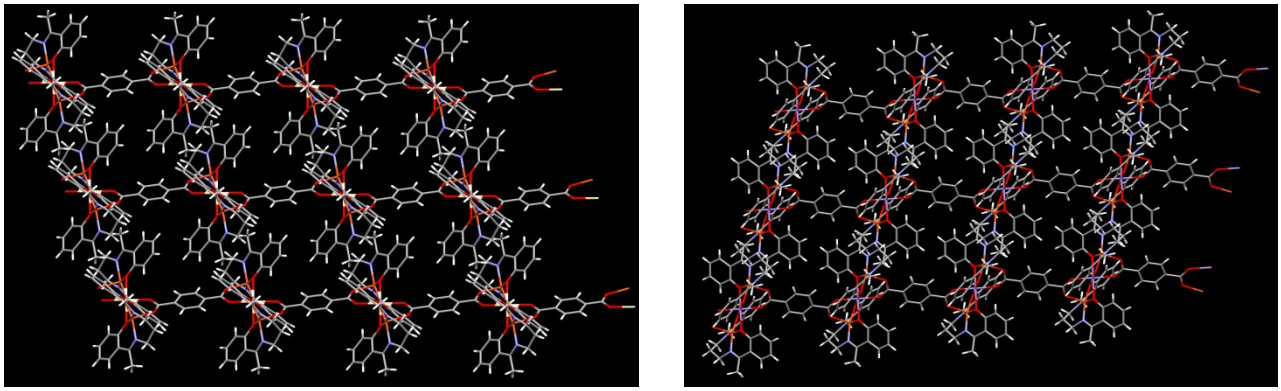

Fig. S14. Representative crystal packing structures of complexes **1** and **2**. Solvent water molecules are not shown for clarity.

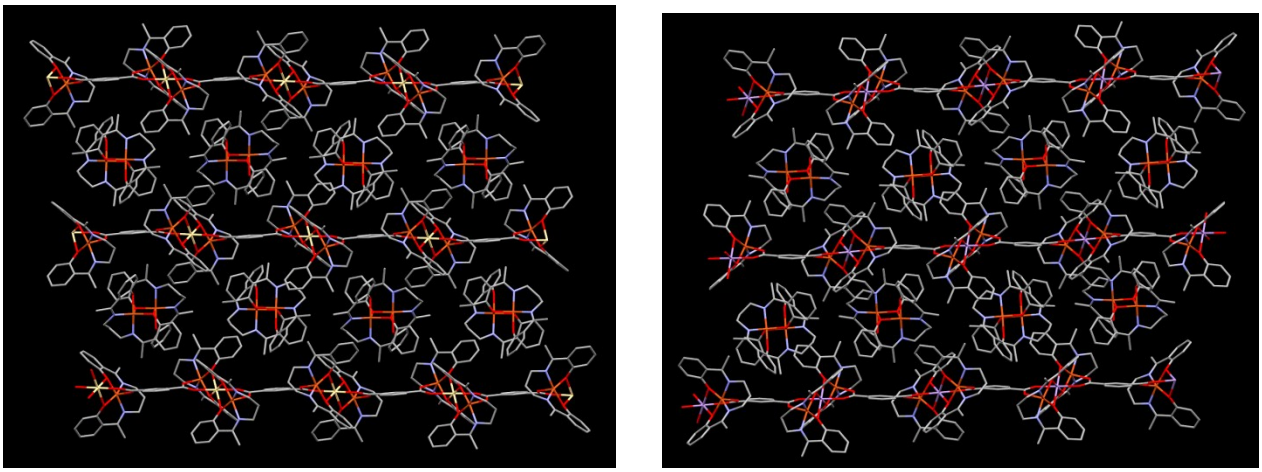

Fig. S15. Representative crystal packing structures of complexes **3** and **4**. H atoms are not shown for clarity.

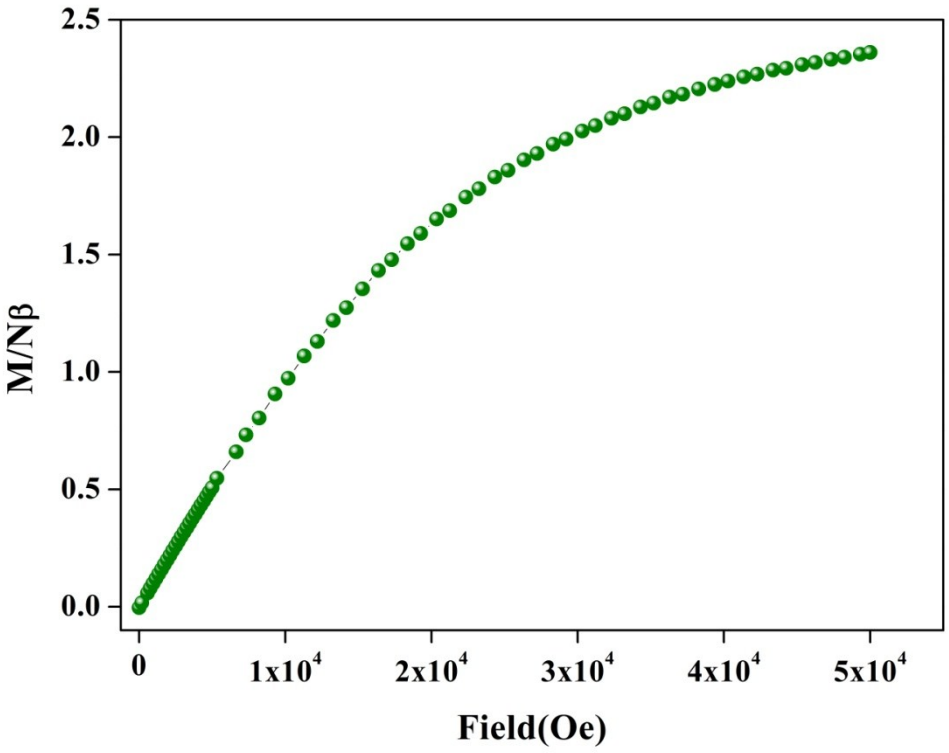

Fig. S16. Isothermal magnetizations at 2.5 K for complex **2**.

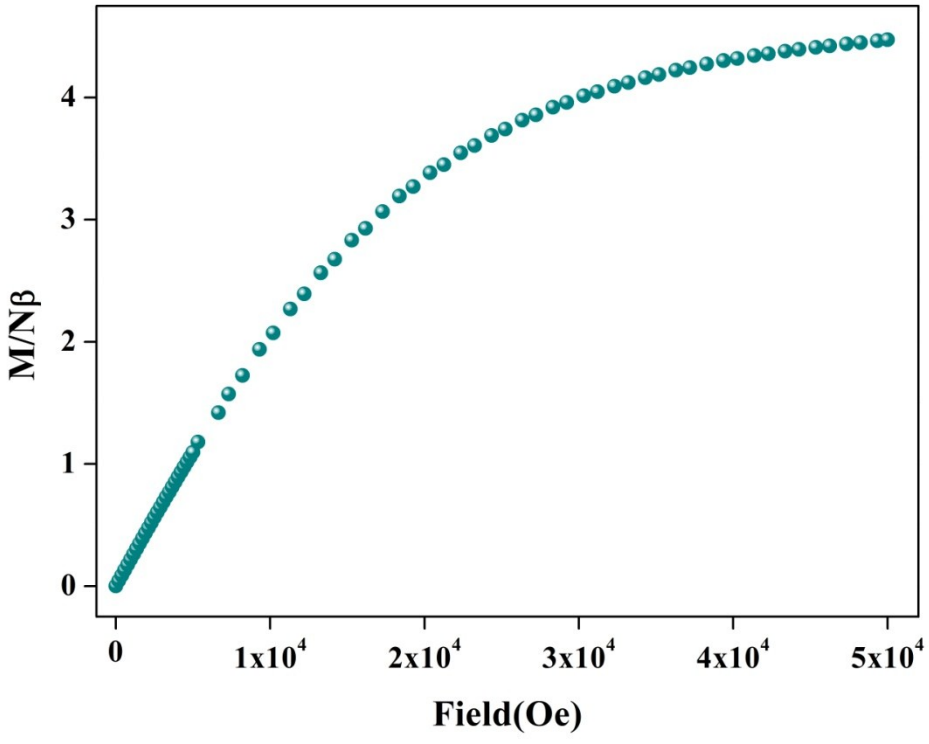

Fig. S17. Isothermal magnetizations at 5 K for complex **4**.

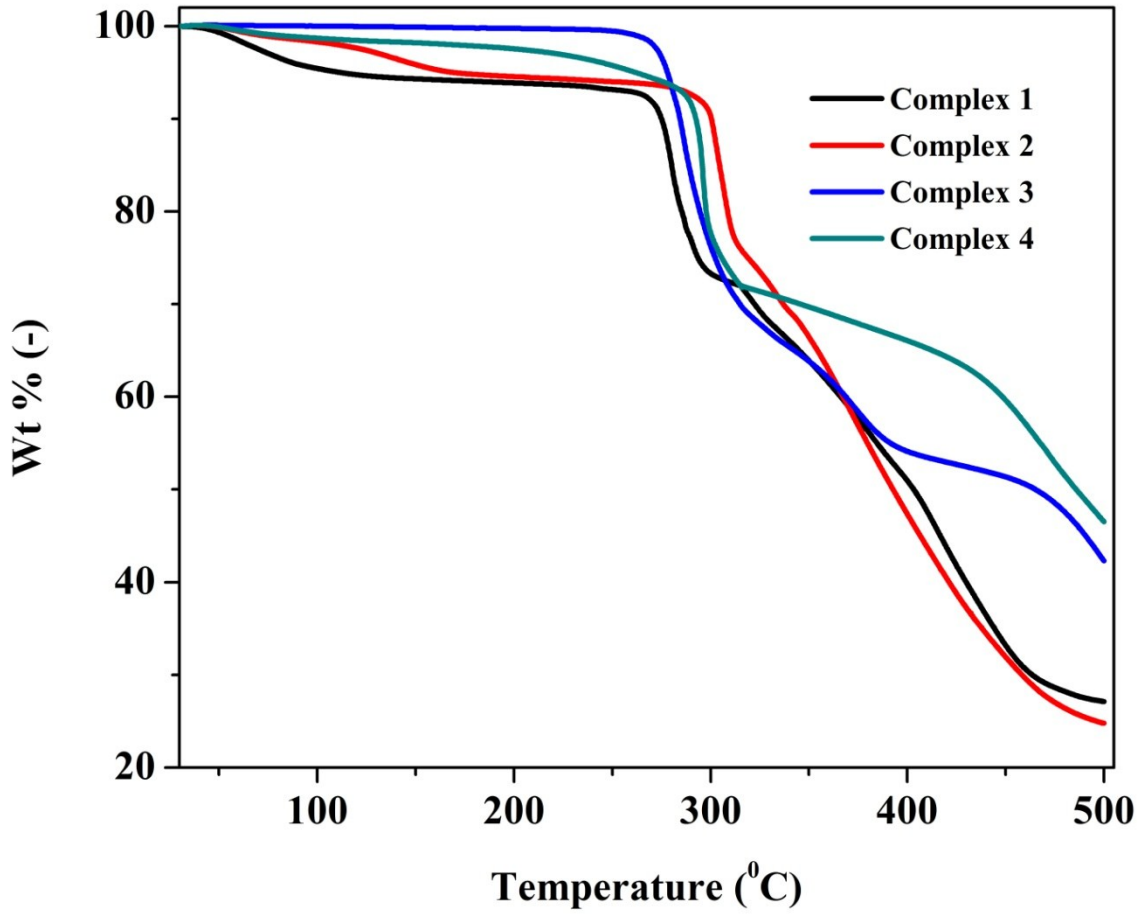

Fig. S18. Thermogravimetric analysis (TGA) plot for complexes **1-4**.

Table S1. Bond distances (Å) and angles (°) for complexes **1** and **2**.

	1	**2**
Cu(1)–O(1)	1.952(5)	1.961(7)
Cu(1)–O(2)	2.177(5)	2.165(8)
Cu(1)–N(1)	2.002(6)	1.978(9)
M(1)–O(1)	2.346(5)	2.238(7)
M(1)–O(3)	2.232(6)	2.123(8)
O(1)–Cu(1)–O(2)	92.1(2)	92.8(3)
O(1)–Cu(1)–N(1)	89.6(2)	90.0(3)
O(1)–Cu(1)–O(1)[a]	84.8(2)	83.7(3)
O(1)–Cu(1)–N(1)[a]	168.2(2)	167.3(3)
O(2)–Cu(1)–N(1)	98.5(2)	98.6(3)
N(1)–Cu(1)–N(1)[a]	93.9(2)	94.0(4)
O(1)–M(1)–O(3)	87.5(2)	88.2(3)
O(1)–M(1)–O(1)[b]	111.7(2)	108.4(2)
O(1)–M(1)–O(1)[c]	180	180
O(1)–M(1)–O(1)[a]	68.3(2)	71.6(2)
O(1)[a]–M(1)–O(3)	92.5(2)	91.9(3)
O(3)–M(1)–O(3)[b]	180	180
M(1)–O(1)–Cu(1)	99.3(2)	98.4(2)

(**1**) : [a] $= x, -y, z$, [b] $= 2-x, y, 2-z$, [c] $= 2-x, -y, 2-z$.

(**2**) : [a] $= x, 1-y, z$, [b] $= 1-x, y, 1-z$, [c] $= 1-x, 1-y, 1-z$.

Table S2. Bond distances (Å) and angles (°) for complexes **3** and **4**.

	3	**4**
Cu(1)–O(1)	1.979(2)	1.929(4)
Cu(1)–O(2)	1.935(2)	1.977(4)
Cu(1)–O(3)	2.183(2)	2.162(4)
Cu(1)–N(1)	1.978(2)	1.989(4)
Cu(1)–N(2)	1.994(2)	1.956(5)
Cu(2)–O(5)	1.925(2)	1.924(4)
Cu(2)–O(5)^{c}	2.538(2)	2.512(4)
Cu(2)–N(3)	1.987(2)	1.958(6)
Cu(2)–N(4)	1.972(3)	1.980(5)
Cu(2)–O(6)	1.908(2)	1.898(4)
M(1)–O(1)	2.295(2)	2.236(4)
M(1)–O(2)	2.331(2)	2.189(4)
O(1)–M(1)–O(2)	71.4(6)	73.8(2)
O(1)–M(1)–O(4)	86.9(6)	89.3 (2)
O(1)–M(1)–O(1)^{a}	180	180
O(1)–M(1)–O(2)^{a}	108.6(6)	106.2(2)
O(1)–M(1)–O(4)^{a}	93.1(6)	90.8(2)
O(2)–M(1)–O(2)^{a}	180	180
O(2)–M(1)–O(4)	88.1(6)	87.6 (2)
O(2)–M(1)–O(4)^{a}	91.9(6)	92.4 (2)
O(4)–M(1)–O(4)^{a}	180	180
O(1)–Cu(1)–O(2)	87.2(7)	85.8(2)
O(1)–Cu(1)–O(3)	92.5(7)	91.1(2)
O(1)–Cu(1)–N(1)	88.8(8)	89.3 (2)
O(1)–Cu(1)–N(2)	159.2(8)	172.6(2)
O(2)–Cu(1)–O(3)	90.5(7)	93.2(2)
O(2)–Cu(1)–N(1)	173.1(9)	159.5(2)
O(2)–Cu(1)–N(2)	88.8(8)	89.9 (2)
O(3)–Cu(1)–N(1)	95.2(7)	106.8 (2)
O(3)–Cu(1)–N(2)	107.8(9)	95.3(2)
N(1)–Cu(1)–N(2)	92.9(8)	92.7(2)
O(5)^{c}–Cu(2)–N(3)	117.8(8)	85.4(2)
O(5)^{c}–Cu(2)–N(4)	85.8(8)	119.0(2)
O(5)–Cu(2)–N(4)	90.4(9)	155.5(2)
O(5)–Cu(2)–O(5)^{c}	86.0(7)	85.5 (2)
O(6)–Cu(2)–N(3)	87.2(1)	174.3(2)
O(6)–Cu(2)–N(4)	175.0(9)	87.5(2)
O(5)^{c}–Cu(2)–O(6)	89.6(8)	89.5 (2)
O(5)–Cu(2)–O(6)	91.3(9)	91.3(2)

O(5)–Cu(2)–N(3)	156.1(9)	90.7(2)
N(3)–Cu(2)–N(4)	93.1(1)	92.9(2)

(**3**) : [a] = 1 – *x* , 1 – *y*, 2 – *z* ; [c] = 1/2 – *x* , 3/2 – *y* ,1 – *z*.(**4**) : [a] =1 – *x* ,1 – *y* ,1 – *z* ; [c] =3/2 – *x* , 3/2 – *y* ,1 – *z*. **M** = Cd (for complexes **1** and **3**) and Mn (for complexes **2** and **4**)

Table S3. The crystal structures of similar compounds containing $(CuL)_2M$ moiety forming supramolecular chain reported in literature.

Complex	**Linker**	**Ref.**
$\{[(CuL)_2Cd(\mu_{1,5}\text{-}N(CN)_2)](ClO_4)\}_n$	Dicyanamide	21(a)
$[\{(CuL)_2Co(m\text{-}BDC)\}\cdot CH_3OH]_\infty$	Isophthalic acid	5(b)
$[\{(CuL)_2Co(p\text{-}BDC)\}\cdot 2CH_3OH]_\infty$	Terephthalic acid	5(b)
$[(CuL^2)_2Co(tph)]_n.2nH_2O$	Terephthalic acid	21(b)
$\{[(CuL)_2Tb(NO_3)_3bpy]\cdot MeOH\cdot 2H_2O\}_\infty$	Bipyridine	21(c)
$(C_{40}H_{36}Co_1Cu_2N_{10}O_4)_n$	Bipyridine	21(d)
$(C_{40}H_{36}Cu_2N_{10}Ni_1O_4)_n$	Bipyridine	21(d)
$(C_{40}H_{36}Cu_2N_{10}O_4Zn_1)_n$	Bipyridine	21(d)
$\{[(CuL)_2Cd(p\text{-}BDC)]\cdot H_2O\}_n$ (**1**)	Terephthalic acid	This work
$\{[(CuL)_2Mn(p\text{-}BDC)]\cdot H_2O\}_n$ (**2**)	Terephthalic acid	This work
$\{[(CuL)_2Cd(m\text{-}BDC)][(CuL)_2]\}_n$ (**3**)	Isophthalic acid	This work
$\{[(CuL)_2Mn(m\text{-}BDC)][(CuL)_2]\}_n$ (**4**)	Isophthalic acid	This work